Harvesting Water Wave Energy by Asymmetric Screening of Electrostatic Charges on a Nanostructured Hydrophobic Thin-Film Surface

Guang Zhu,[†,‡,#] Yuanjie Su,[‡,#] Peng Bai,[‡] Jun Chen,[‡] Qingshen Jing,[‡] Weiqing Yang,[‡] and Zhong Lin Wang[†,‡,*]

[†]Beijing Institute of Nanoenergy and Nanosystems, Chinese Academy of Sciences, Beijing 100083, China and [‡]School of Materials Science and Engineering, Georgia Institute of Technology, Atlanta, Georgia 30332, United States. [#]G. Zhu and Y. Su contributed equally.

ABSTRACT Energy harvesting from ambient water motions is a desirable but underexplored solution to on-site energy demand for self-powered electronics. Here we report a liquid–solid electrification-enabled generator based on a fluorinated ethylene propylene thin film, below which an array of electrodes are fabricated. The surface of the thin film is charged first due to the water–solid contact electrification. Aligned nanowires created on the thin film make it hydrophobic and also increase the surface area. Then the asymmetric screening to the surface charges by the waving water during emerging and submerging processes causes the free electrons on the electrodes to flow through an external load, resulting in power generation. The generator produces sufficient output power for driving an array of small electronics during direct interaction with water bodies, including surface waves and falling drops. Polymer-nanowire-based surface modification increases the contact area at the liquid–solid interface, leading to enhanced surface charging density and thus electric output at an efficiency of 7.7%. Our planar-structured generator features an all-in-one design without separate and movable components for capturing and transmitting mechanical energy. It has extremely lightweight and small volume, making it a portable, flexible, and convenient power solution that can be applied on the ocean/river surface, at coastal/offshore areas, and even in rainy places. Considering the demonstrated scalability, it can also be possibly used in large-scale energy generation if layers of planar sheets are connected into a network.

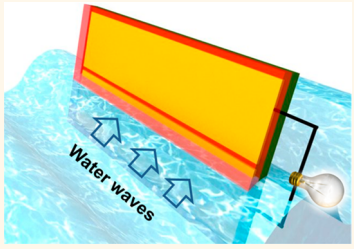

KEYWORDS: energy harvesting · water waves · contact electrification · generators · self-powered electronics

Ambient water motions, presenting in the form of river flows, ocean tides and waves, and even rain drops, contain a gigantic reserve of renewable mechanical energy. Taking advantage of this energy has major significance in grid-level energy generation by large-scale power plants for public utilities in order to relieve our sole reliance on limited fossil fuels.[1,2] Moreover, it also provides a viable route to fulfilling on-site power demand for long-term operation of self-powered autonomous systems, such as off-grid and stand-alone facilities, or remote sensor networks.[3−6] Most previously demonstrated converters for water motions depended on normal electromagnetic generators[7−10] that were bulky and heavy in order to obtain decent output power and conversion efficiency.[11] Besides, they usually required other essential components,[2] such as an absorber to collect ambient water motions and a turbine to drive the generator, which further expanded the size of the system and added complexity as well as cost. Moreover, natural water motions, especially waves, can be categorized into a number of forms, and not all of them are suitable for driving a turbine.[2] Therefore, a small-sized, lightweight, cost-effective, and all-in-one approach that can directly interact with water bodies is greatly desirable as a key to solving the above problems.

Initial efforts in this regard included flexible piezoelectric strips (so-called "eels")[12−14] that undulated in water flow as driven by vortices shed from an upstream bluff body, and a low-dimensional carbon nanostructure, *e.g.*, carbon nanotubes[15,16] and few-layered graphene,[17] over which voltages were induced when polar liquids flowed. In the former design, reciprocating-strained eels posed a major challenge to prolonged operation

* Address correspondence to zhong.wang@mse.gatech.edu.

Received for review March 4, 2014 and accepted April 15, 2014.

Published online 10.1021/nn5012732

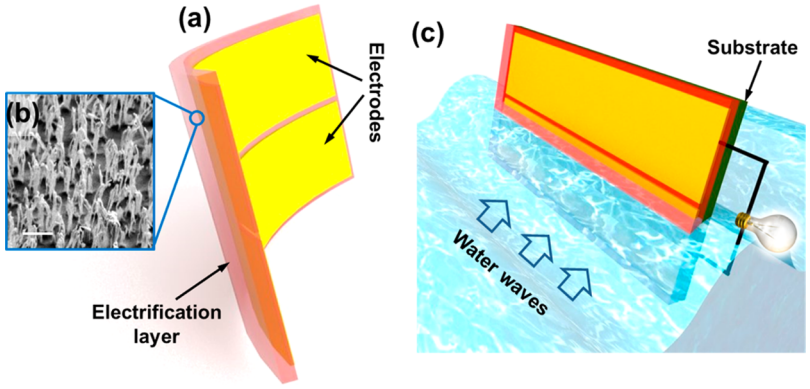

Figure 1. Structural design of the LSEG. (a) Schematic of the bent electrification layer with two electrodes on one side. (b) SEM image (tilting angle of 30°) of the polymer nanowires on the opposite side of the polymer layer. The scale bar is 1 μm. (c) Schematic of a substrate-supported LSEG positioned in water waves. The up-and-down movement of the surrounding water body induces electricity generated between the two electrodes.

due to mechanical fatigue especially of electrodes, while the latter was restricted by materials availability and by ion concentrations in water.[17] Besides, both of them harnessed only constant water currents, leaving other forms of water motions largely intact.

Herein we report a liquid–solid electrification-enabled generator (LSEG) for harvesting energy from a variety of water motions. Coupled with electrostatic induction, surface triboelectric charges resulting from interaction with water induce free electrons to flow alternatingly between electrodes as the device has a repeatedly varying contact area with the surrounding water body. Having a planar structure (6 cm by 3 cm by 50 μm), one layer of the LSEG generates an optimum average output power of 0.12 mW at a relative velocity of 0.5 m/s. Nanowire-based modification from polymer nanowires plays a key role in obtaining such an output power. The all-in-one LSEG does not require extra mechanical components for capturing or transmitting mechanical motions, and its stationary and strain-free design has electrodes fully imbedded and secured without any movable parts, which ensures its durability and reliability for long-term operation. Made from conventional polymeric materials, it is highly cost-effective and easily scalable in size. An integrated LSEG with an array of electrodes is demonstrated as a power source for tens of LED bulbs by harvesting ambient energy from a waving water surface and even falling water drops, explicitly demonstrating the potential of deploying the LSEG on the ocean/river surface, at coastal/offshore areas, and even in rainy places for applications such as monitoring, surveillance, and navigation.

RESULTS AND DISCUSSION

A basic unit of the LSEG is sketched in Figure 1a. On one side of a fluorinated ethylene propylene (FEP) thin film, two parallel strip-shaped electrodes are fabricated, which are discrete with a fine gap in between. The other side of the FEP layer, modified to intentionally create patterned surface roughness at the nanoscale (Figure 1b), directly interacts with ambient water to generate surface triboelectric charges at the liquid–solid interface. The vertically aligned nanowires, ~100 nm in diameter and ~2 μm in length, are for promoting the output power of the LSEG by enhancing the contact area with water. The FEP is chosen for a number of reasons. Foremost, it is the most negative material that is commercially available with respect to triboelectric polarity,[18–20] which enables superior surface charging ability compared with other materials. In addition, other advantageous features, including heat resistance, radiation stability, and chemical inertness, make the FEP a desirable and durable material for underwater operation. The fabricated layer is then applied onto a substrate (Figure 1c) for quantitative measurement. The detailed fabrication process is presented in the Methods section.

The operation of the LSEG relies on a repetitive emerging–submerging process with traveling water waves (Figure 1c), in which the coupling between triboelectrification and electrostatic induction gives rise to alternating flows of electrons between electrodes. It was previously reported that contact electrification between a triboelectrically negative material, *e.g.*, a fluorinated polymer, and water generated surface triboelectric charges at the contact interface[21–24] with negative charges on the solid surface. Generally, this charging phenomenon was explained using an interfacial electrical double-layer model, which took into account the ions in the liquid adsorbed onto the solid surface. It needs pointing out that some important fundamentals of the physical mechanism are still elusive, including the real identity of the surface charging species.[23,24] What we do know is that after interacting with water the FEP surface retains a layer of negative surface charges that do not dissipate in an extended period of time (Figure 2a). The nanowires fabricated on the surface of the film make it hydrophobic so that water is repelled immediately after the

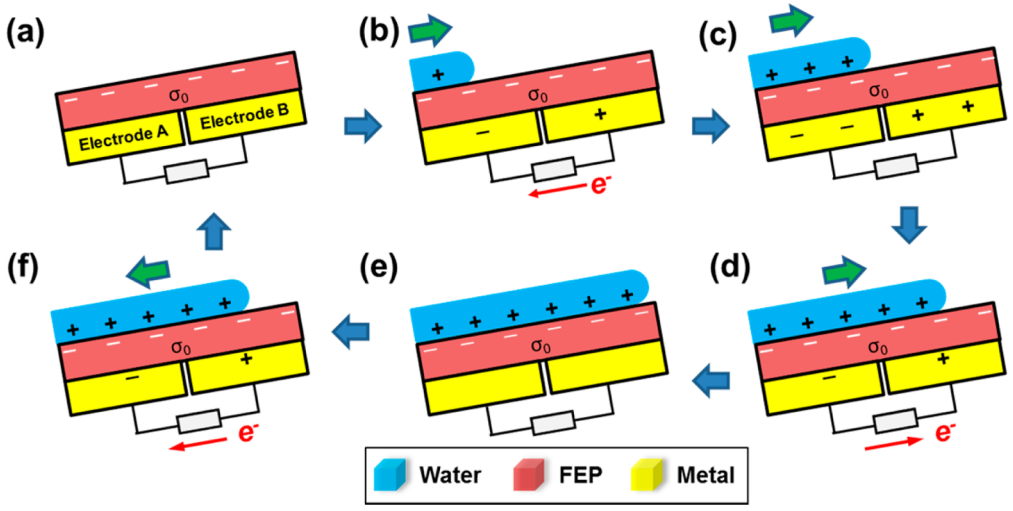

Figure 2. Electricity-generating process of the LSEG. (a) The entire device is exposed without water. (b) Electrode A is partically submerged as a result of the rising water wave. Free electrons are induced from electrode B to electrode A. (c) The water surface levels with the middle point of the device. (d) Electrode B is being covered by water. Free electrons flow back to electrode B. (e) The entire device is completely submerged. (f) The wave is receding, making electrode B partially exposed.

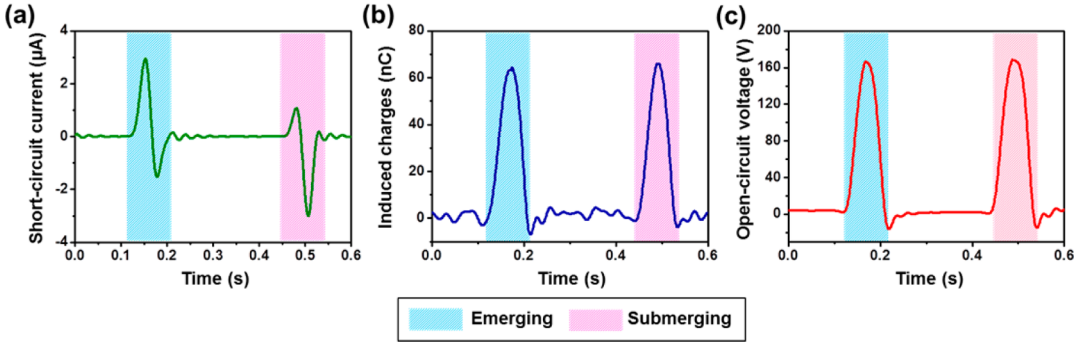

Figure 3. Electric measurement results as the LSEG is repetitively submerged at a moving velocity of 0.5 m/s. (a) Short-circuit current. (b) Induced charges without extra load between electrodes. (c) Open-circuit voltage.

descending of the water surface. Once electrode A is partially submerged by the rising water wave, positive charges in water (such as hydroxonium) screen the negative triboelectric charges on the FEP surface by forming an interfacial electrical double layer. As a result, the unbalanced electric potential between the two electrodes due to the asymmetric distribution of charges drives free electrons to flow from electrode B to electrode A until the device is submerged halfway. Figure 2c then corresponds to the state with the maximum quantity of induced charges on the electrodes. As electrode B starts to sink into the water, induced electrons flow back to electrode B because the electric potential distribution varies toward equilibrium (Figure 2d). Finally, when the device is completely covered by water, triboelectric charges are entirely screened. Consequently, all induced charges vanish (Figure 2e), similar to the state in Figure 2a. If the wave then recedes, another alternating cycle of the current is then produced (Figure 2f). Therefore, the generated electricity is attributed to the sequential process of contact electrification and asymmetric-screening-enabled electrostatic induction.

For quantitative measurement, relative motion between the LSEG and water was achieved by a linear electric motor that drove the LSEG to produce a reciprocating motion at controlled velocities (see Methods). Here, regular tap water was used. As shown in Figure 3a, the short-circuit current (I_{sc}) has an alternating behavior with an amplitude of 3 μA at a velocity of 0.5 m/s. The total amount of induced charges in one cycle reaches 75 nC (Figure 3b).

In open-circuit condition, electrons cannot transfer between electrodes. During interaction with water, the open-circuit voltage (V_{oc}), defined as the electric potential difference between the two electrodes, remains 0 at both the emerged (Figure 2a) and submerged states (Figure 2e). It reaches the maximum when the water surface levels with the middle point of the generator (Figure 2c). On the basis of the model of infinitely large charged planes without consideration

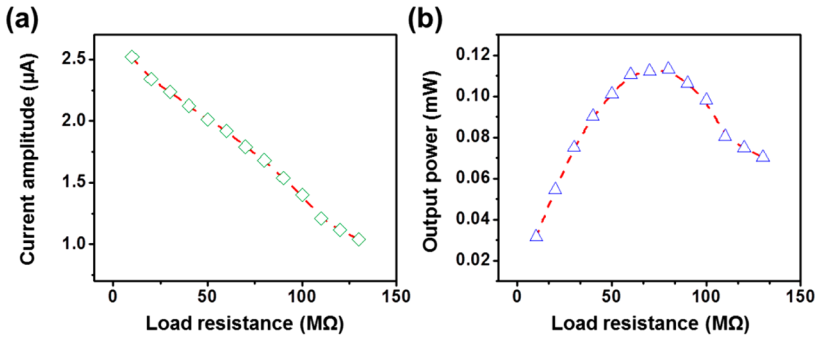

Figure 4. Electric measurement results of load matching test as the LSEG is repetitively submerged at a moving velocity of 0.5 m/s. (a) Amplitude of current with increasing load resistance between electrodes. (b) Average output power with increasing load resistance between electrodes.

of edge effects,[25,26] the V_{oc} can be analytical expressed by the following equation.

$$V_{oc} = \frac{d\sigma_0}{\varepsilon_0 \varepsilon_r} \quad (1)$$

where d is the thickness of the FEP layer, σ_0 is the triboelectric charge density on top of the FEP layer as a constant, ε_0 is the dielectric constant of vacuum, and ε_r is the relative dielectric constant of FEP. Figure 3c shows the measured V_{oc} that oscillates between 0 and the maximum value of 160 V at a velocity of 0.5 m/s. By submitting the measured induced charges into eq 1 (d = 75 μm, $\sigma \approx 42$ μC/m^2, ε_r = 2.1), the peak-to-peak value of the V_{oc} is theoretically calculated to be ~168 V, which agrees well with the experimentally measured value. Control groups using other thin-film materials that had inferior triboelectric negativity yielded reduced electric output, and relative magnitudes among different devices followed the material's triboelectric negativity of the electrification layer (Supporting Figure S1), which thus further supported the proposed operating principle.

Once an external load is applied, the amplitude of the output current drops as the load resistance increases, as shown in Figure 4a. Here, the average output power is defined by the following equation:

$$W = I_{rms}^2 R \quad (3)$$

where I_{rms} is the root mean value of the current amplitude, and R is the external load resistance. As shown in Figure 4b, the average output power reaches the optimum value of 0.12 mW at the matched load of 80 MΩ. The energy conversion efficiency of this device is calculated to be around 7.7%. The detailed analysis is presented in the Supporting Information.

Here, three categories of factors were investigated to determine how to tune the electric output of the LSEG, *i.e.*, velocity of the relative movement, aspect ratio of the device, and ion concentration of the water body.

First, relative velocity is a major factor that influences the electric output. It is interesting to notice that both the V_{oc} and induced charges have an approximately linear relationship with the velocity, respectively, as revealed in Figure 5a and b. The induced charges both increase by around 100% as the velocity increases from 0.1 to 0.5 m/s, which is possibly attributed to velocity-dependent surface charging density. More triboelectric charges are generated on the FEP surface if a more dynamic interaction with the water is involved, which was observed in previous studies on electrification between a fluorinated polymer and water.[23,24] Further systematic investigations on the kinetics of the charge-generation process are needed to provide more insights into the velocity-dependent electric output. The current amplitude is determined by two factors, that is, charge quantity and velocity. When both of the factors increase, the current rises at an increasing rate, as shown in Figure 5c.

Second, design parameters, especially the aspect ratio of the device, also have a decisive effect on the electric output of the LSEG. On the basis of previous studies,[23,24] it was observed that pre-existing charges in the water can influence subsequent charge transfer with a solid surface. Specifically, the water may have a weaker ability to charge the solid surface once it already carries opposite charges. Here in our measurement, the LSEG was driven by a linear motor in order to slide relative to the static water body. As a result, it is the surface part of the water that actually has the charge transfer with the LSEG surface. Once the LSEG starts to dip into the water, the surface part of the water is positively charged instantaneously. Subsequent electrification as the LSEG continues to dip will become weaker due to the increasing pre-existing positive charges in the water. Therefore, it is very likely that the top part of the LSEG may have a lower surface charging density compared to the bottom part. Given that the area is fixed, a narrower LSEG with a higher aspect ratio has a shorter interaction distance with the water, more surface triboelectric charges, and thus higher electric output accordingly, as illustrated by the increasing V_{oc} and induced charges in Figure 5d and e, respectively. It is noticed that the I_{sc} is again

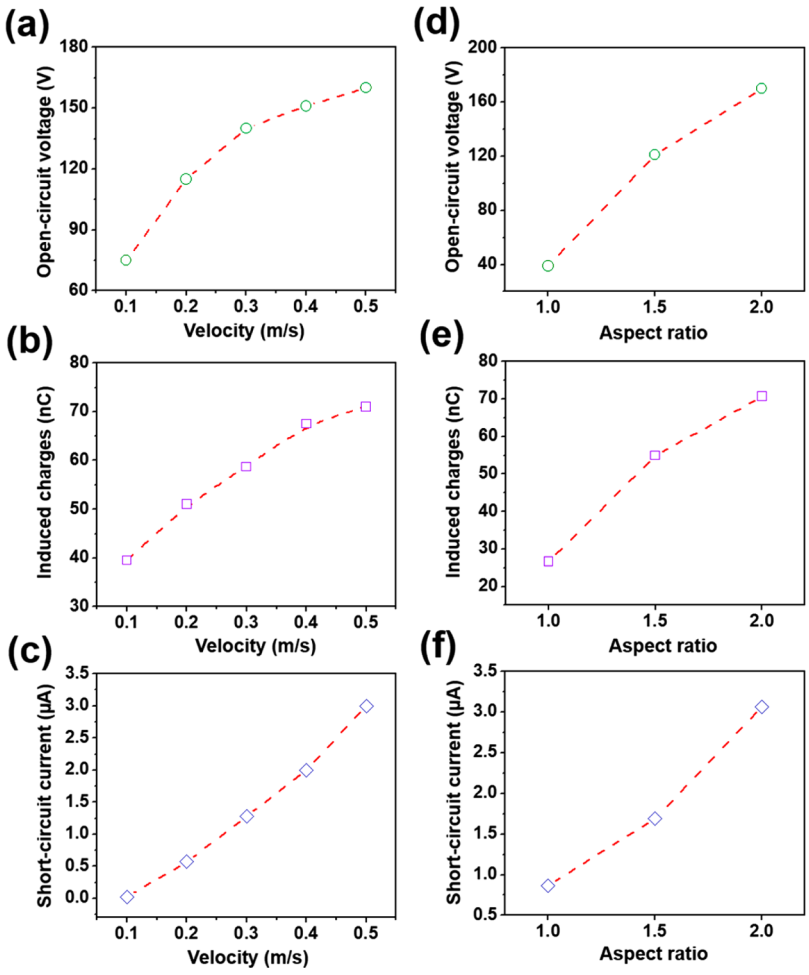

Figure 5. Electric measurement results on factors that influence the electric output. (a) Open-circuit voltage with increasing velocity. (b) Induced charges with increasing velocity. (c) Short-circuit current with increasing velocity. (d) Open-circuit voltage with increasing aspect ratio of the device. (e) Induced charges with increasing aspect ratio of the device. (f) Short-circuit current with increasing aspect ratio of the device.

influenced to a larger extent, which is indicated by the positive curvature in Figure 5f. Therefore, fine features of the electrode play a key role in designing a high-performance LSEG.

Third, ion concentration or conductivity of the water body also plays an important role. In a control experiment, the tap water was replaced by a saturated sodium chloride solution with an extremely high concentration of ions. Induced charges 40% lower than that in Figure 5b were obtained with the same device as well as the same moving velocity. This is because a low ion concentration assists generation of the triboelectric charges, while a high concentration has the opposite effect.[21] Even with the highest possible concentration, the LSEG can still provide an electric output power, although at a mildly reduced magnitude, which is an indicator of true applicability of our device in natural water bodies.

In addition, the effect of the nanostructured surface modification is clear in that devices with the nanowires provide an average enhancement in induced charges by 50% in comparison to those without the modification. Here, the nanostructured LSEG surface interacts between the bulk water body instead of a single static water droplet, and the dynamic interaction involves kinetic energy due to the nonstop emerging and submerging processes. As a result, the water can infiltrate, at least largely if not completely, into the aligned nanowires even though they are hydrophobic. Then, higher surface contact area and enhanced electric output can be obtained.

Instead of being driven by an electric motor for quantitative measurement, an integrated LSEG (I-LSEG) with a scaled-up design was further tested in a normal environment where energy from ambient water motions was harvested. The I-LSEG consists of six strip-shaped electrodes with each having lateral dimensions of 20 cm by 6 mm (Supporting Figure S2). Then, a total of five basic units were formed by any pair of adjacent electrodes. The electric output of each pair was first rectified through an electric bridge and then constructively superimposed through a parallel connection. In the first demonstration, the I-LSEG was vertically fixed in a water container with a tilting angle of

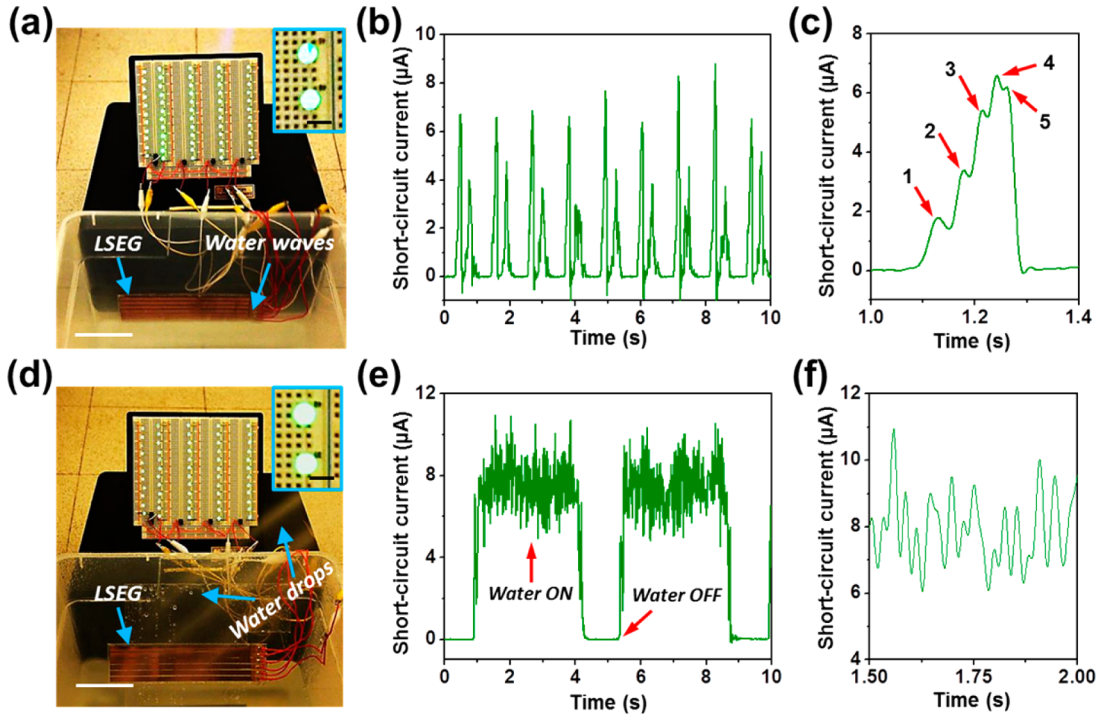

Figure 6. Demonstrations of the LSEG in harvesting energy from ambient water motions. (a) Demonstration of an integrated LSEG with an array of electrode in powering tens of LED bulbs by harnessing water waves. The scale bar is 8 cm. Inset: Zoom-in view of two lit LEDs. (b) Short-circuit current of the integrated LSEG when it interacts with water waves at a frequency of ~0.7 Hz. (c) Zoom-in view of a large current peak. (d) Demonstration of the integrated LSEG in powering tens of LED bulbs by harnessing water drops. The scale bar is 8 cm. Inset: Zoom-in view of two lit LEDs. (e) Short-circuit current of the integrated LSEG when it interacts with falling water drops. (f) Zoom-in view of the current signal when water drops are shed upon the device.

30° away from the vertical position. The water surface leveled with the lower edge of the device (Supporting Figure S2). The container was then gently tilted back and forth to create traveling waves that washed the I-LSEG in a reciprocating way, similar to the circumstance along the seashore and riverbanks. Pulses of dc current are produced, as shown in Figure 6b. A zoomed-in view of a single current pulse in Figure 6c reveals multiple peaks. Since the five units interact with the water sequentially instead of simultaneously, they result in five current pulses that merge together but with timing mismatch. The generated electricity could light up tens of LED bulbs, proving the capability of the LSEG as a power source for electronics (Figure 6a, Supporting Movie 1). This demonstration clearly indicates that our device can be potentially used along the seaside/riverside area. Besides, accompanied with a buoy, the LSEG can also be possibly deployed offshore on the ocean surface.

In light of the operating principle that requires only changing of the contact area with water, we further demonstrated energy harvesting from falling water or rain drops. The I-LSEG was still braced with the same tilting angle (Figure 6d). A sprinkler head was used to spray water onto the device. As the water accumulated, droplets slid across the I-LSEG surface perpendicular to the electrode array. Since a moving droplet could momentarily cover part of the device, electricity was generated as the droplet crossed boundaries between adjacent electrodes. With numerous droplets, a large number of current pulses merged together, leading to an apparent continuous dc output (Figure 6e and f). Larger water droplets tend to create more fluctuation in the output current but do not greatly change the overall performance. The electric output was again sufficient to power the LED bulbs (Figure 6d, Supporting Movie 2). This demonstration further expands the applicability of the LSEG, providing a new means of energy harvesting from a largely unexploited energy source, namely, natural precipitation.

CONCLUSION

In summary, we developed a single-component energy converter that was made from thin-film materials. Without having any movable components, it generated electricity through triboelectric effect at the solid−liquid interface when directly interacting with ambient water bodies, showing a practically feasible technology for harvesting part of the wave energy. Shrinking down the width feature of the electrodes and modifying the surface morphology with nanowires could substantially boost the electric output. Integrating an array of units on a single substrate, it was easily scalable in size and demonstrated energy harvesting from ambient water waves

and drops for directly powering electronics, showing potential applications of the LSEG onshore/offshore and even in rainy areas. Due to its planar two-dimensional design, further integration into a multilayered structure is also possible for large-scale power generation.

METHODS

Fabrication of the LSEG. A 75 μm-thick FEP film was prepared with the desired dimensions. A hollow mask made from by a 1.5 mm-thick acrylic sheet was prepared through precision laser cutting. The mask had through patterns that were the same as electrodes. The number and density of electrodes were solely determined by the mask. Then the mask was mounted on to the FEP film. E-beam evaporation was used to deposit a copper layer (200 nm) onto the exposed FEP surface. Lead wires were connected to the electrodes as output terminals with one-to-one correspondence. Subsequently, the film was attached to a substrate with the assistance of adhesive with the electrode layer imbedded underneath. Finally, the entire device went through plasma etching to create vertically aligned nanowires on the top surface. The technical details of the etching were previously reported.[27]

Experimental Setup for Quantitative Measurement. A fabricated LSEG was attached to a vertically mounted linear motor. The moving direction of the motor was perpendicular to the array of strip-shaped electrodes. A container filled with tap water was placed under the device with the water level adjacent to the device edge. Then reciprocating motion of the generator was achieved through the motor-controlling program.

Conflict of Interest: The authors declare no competing financial interest.

Acknowledgment. Research was supported by U.S. Department of Energy, Office of Basic Energy Sciences (award DE-FG02-07ER46394), and the "Thousands Talents" Program for Pioneer Researcher and His Innovation Team, China, Beijing City Committee of Science and Technology (projects Z131100006013004, Z131100006013005). Patents have been filed based on the research results presented in this article.

Supporting Information Available: More detailed information about the comparison on LSEGs fabricated by different materials and the actual setup for application demonstrations of the integrated LSEG. This material is available free of charge *via* the Internet at http://pubs.acs.org.

REFERENCES AND NOTES

1. Boyle, G. *Renewable Energy: Power for a Sustainable Future*; Oxford University Press: Oxford, 1996.
2. Khaligh, A.; Onar, O. C. *Energy Harvesting Solar, Wind, and Ocean Energy Conversion Systems*; CRC Press: Boca Raton, 2009.
3. Muetze, A.; Vining, J. G. Ocean Wave Energy Conversion-A Survey. *41st Industry Applications Society Annual Meeting*; 2006.
4. Scruggs, J.; Jacob, P. Harvesting Ocean Wave Energy. *Science* **2009**, *323*, 1776–1779.
5. Murray, R.; Rastegar, J. Novel Two-Stage Piezoelectric-Based Ocean Wave Energy Harvesters for Moored or Unmoored Buoys. *Proc. SPIE* **2009**, *7288*, 72880E (1)–7280E (12).
6. Kornbluh, R. D.; Pelrine, R.; Prahlad, H.; Wong-Foy, A.; McCoy, B.; Kim, S.; Eckerle, J.; Low, T. From Boots to Buoys: Promise and Challenges of Dielectric Elastomer Energy Harvesting. *Proc. SPIE* **2011**, *7976*, 797605 (1)–797605 (19).
7. Jouanne, V. A. Harvesting the Waves. *Mech. Eng. Mag.* **2006**, *128*, 24–27.
8. Henderson, R. Design, Simulation, and Testing of a Novel Hydraulic Power Take-Off System for the Pelamis Wave Energy Converter. *Renew. Energy* **2006**, *31*, 271–283.
9. Drouen, L.; Charpentier, J. F.; Semail, E.; Clenet, S. Study of an Innovative Electrical Machine Fitted to Marine Current Turbines. *Proc. Oceans 2007 Eur.* **2007**, *18—21*, 1–6.
10. Wolfbrandt, A. Automated Design of a Linear Generator for Wave Energy Converters-A Simplified Model. *IEEE Trans. Magn.* **2007**, *42*, 1812–1819.
11. Beeby, S.; White, N. *Energy Harvesting for Autonomous Systems*; Artech House: Norwood, 2010.
12. Allen, J. J.; Smits, A. J. Energy Harvesting Eel. *J. Fluid. Struct.* **2001**, *15*, 629–640.
13. Taylor, G. W.; Burns, J. R.; Kammann, S. M.; Power, W. B.; Welsh, T. R. The Energy Harvesting Eel: a Small Subsurface Ocean/River Power Generator. *IEEE J. Ocean. Eng.* **2001**, *26*, 539–546.
14. Akaydin, H. D.; Elvin, N.; Andreopoulos, Y. Energy Harvesting from Highly Unsteady Fluid Flow Using Piezoelectric Materials. *J. Intell. Mater. Syst. Struct.* **2010**, *21*, 1263–1278.
15. Ghosh, S.; Sood, A. K.; Kumar, N. Carbon Nanotube Flow Sensor. *Science* **2003**, *299*, 1042–1044.
16. Liu, Z.; Zheng, K.; Hu, L.; Liu, J.; Qiu, C.; Zhou, H.; Huang, H.; Yang, H.; Li, M.; Gu, C.; *et al.* Surface-Energy Generator of Single-Walled Carbon Nanotubes and Usage in a Self-Powered System. *Adv. Mater.* **2010**, *22*, 999–1003.
17. Dhiman, P.; Yavari, F.; Mi, X.; Gullapalli, H.; Shi, Y.; Ajayan, P. M.; Koratkar, N. Harvesting Energy from Water Flow over Graphene. *Nano Lett.* **2011**, *11*, 3123–3127.
18. Zhu, G.; Chen, J.; Liu, Y.; Bai, P.; Zhou, Y. S.; Jing, Q.; Pan, C.; Wang, Z. L. Linear-Grating Triboelectric Generator Based on Sliding Electrification. *Nano Lett.* **2013**, *13*, 2282–2289.
19. Greason, W. D.; Oltean, L. M.; Kucerosvky, Z.; Ieta, A. C. Triboelectric Charging between Polytetrafluoroethylene and Metals. *IEEE Trans. Ind. Appl.* **2004**, *40*, 442–450.
20. Zhou, Y. S.; Liu, Y.; Zhu, G.; Lin, Z.-H.; Pan, C.; Jing, Q.; Wang, Z. L. *In Situ* Quantitative Study of Nanoscale Triboelectrification and Patterning. *Nano Lett.* **2013**, *13*, 2771–2776.
21. Lin, Z.-H.; Cheng, G.; Lin, L.; Lee, S.; Wang, Z. L. Water-Solid Surface Contact Electrification and its Use for Harvesting Liquid Wave Energy. *Angew. Chem., Int. Ed.* **2013**, *52*, 1–6.
22. Ravelo, B.; Deval, F.; Kane, S.; Nsom, B. Demonstration of the Triboelectricity Effect by the Flow of Liquid Water in the Insulating Pipe. *J. Electrostat.* **2011**, *69*, 473–478.
23. Yatsuzuka, K.; Mizuno, Y.; Asano, K. Electrification Phenomenon of Pure Water Droplets Dripping and Sliding on a Polymer Surface. *J. Electrostat.* **1994**, *32*, 157–171.
24. Yatsuzuka, K.; Mizuno, Y.; Asano, K. Electrification of Polymer Caused by Sliding Ultrapure Water. *IEEE Trans. Ind. Appl.* **1996**, *32*, 825–831.
25. Zhu, G.; Pan, C.; Guo, W.; Chen, C.-Y.; Zhou, Y.; Yu, R.; Wang, Z. L. Triboelectric-Generator-Driven Pulse Electrodeposition for Micropatterning. *Nano Lett.* **2012**, *12*, 4960–4965.
26. Zhu, G.; Chen, J.; Zhang, T.; Jing, Q.; Wang, Z. L. Radial-arrayed rotary electrification for high performance triboelectric generator. *Nat. Commun.* **2014**, *5*, 3426.
27. Fang, H.; Wu, W.; Song, J.; Wang, Z. L. Controlled Growth of Aligned Polymer Nanowires. *J. Phys. Chem. C* **2009**, *113*, 16571–16574.